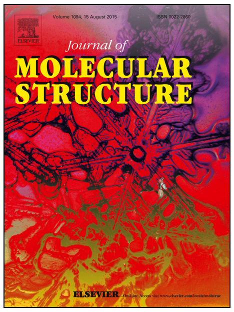

Three new energetic compounds based on 1-amino-2-nitroguanidine (ANQ): synthesis, crystal structure and properties

Zhicun Feng, Xiaoge Guan, Kangzhen Xu, Lianjie Zhai, Fengqi Zhao

PII: S0022-2860(18)30503-9
DOI: 10.1016/j.molstruc.2018.04.061
Reference: MOLSTR 25134

To appear in: *Journal of Molecular Structure*

Received Date: 19 January 2018
Revised Date: 15 April 2018
Accepted Date: 17 April 2018

Please cite this article as: Z. Feng, X. Guan, K. Xu, L. Zhai, F. Zhao, Three new energetic compounds based on 1-amino-2-nitroguanidine (ANQ): synthesis, crystal structure and properties, *Journal of Molecular Structure* (2018), doi: 10.1016/j.molstruc.2018.04.061.

Three new energetic compounds based on 1-amino-2-nitroguanidine (ANQ): synthesis, crystal structure and properties

Zhicun Feng [a], Xiaoge Guan [a], Kangzhen Xu [a,]*, Lianjie Zhai [b], Fengqi Zhao [b]

[a] *School of Chemical Engineering, Northwest University, Xi'an 710069, P. R. China*
[b] *Xi'an Modern Chemistry Research Institute, Xi'an 710065, P. R. China*

Abstract: Three new derivatives of ANQ, 1-(2,4-dinitroanilino)-2-nitroguanidine (DNNG), 1-(2,4,6-trinitroanilino)-2-nitroguanidine (TNNG) and 1-amino-2-nitroguanidine-3,5-dinitrosalicylic salt (ANQ·DNS), were synthesized by the nucleophilic substitution reaction and salt formation reaction. Single crystal structures of TNNG and ANQ·DNS·$3H_2O$ were determined. TNNG crystallizes in the monoclinic crystal system with space group $P2_1/c$ containing four molecules per unit cell, and ANQ·DNS·$3H_2O$ crystallizes in the triclinic crystal system with space group *P*-1 containing two ANQ·DNS·$3H_2O$ units per unit cell. The thermal behaviors, impact sensitivities and detonation properties of the three compounds were studied. DNNG and TNNG possess similar thermal behaviors and both present only one intense exothermic decomposition process at around 170 °C, but ANQ·DNS shows more complex thermal behaviors. ANQ·DNS possesses the lowest impact sensitivity (>40 J), DNNG presents the highest thermal stability (175 ºC), and TNNG shows the best detonation properties (detonation velocity = 8.3 km s^{-1}, detonation pressure = 31.1 GPa). TNNG has potential value of research and application as primary explosives.

Keywords: 1-Amino-2-nitroguanidine (ANQ); Crystal structure; Thermal behavior; Detonation properties

1. Introduction

For many years, guanidine and its derivatives, such as 1-amino-3-nitroguanidine, aminoguanidine and triaminoguanidine, as a kind of important rich-nitrogen high-energy material, have been extensively studied in the field of energetic materials [1-11]. 1-Amino-2-nitroguanidine (ANQ) has been synthesized through the hydrazinolysis reaction of nitroguanidine in aqueous solution since 1920s [12-15]. ANQ, containing an amino and a nitro group in its molecular

---

* Corresponding author at: Northwest University, School of Chemical Engineering, Taibai Road 229, Xi'an 710069, China. Tel.: +86 29 88307755; Fax: +86 29 88302633.
E-mail address: xukz@nwu.edu.cn (K. Xu).

structure, is used as an important explosive and shows relatively good thermal stability with a decomposition temperature of 180 ºC [16]. Furthermore, the detonation performance of ANQ is comparable to that of 1,3,5-trinitroperhydro-1,3,5-triazine (RDX), and the density, detonation velocity (*D*) and detonation pressure (*P*) of ANQ are 1.72 g cm^{-3}, 8729 m s^{-1} and 30.7 GPa respectively, which makes ANQ be a promising energetic material [17-21].

Because of the adjacent amino group and hydrazine group, ANQ possesses high reactivity. Many derivatives of ANQ have been reported, which involves the cyclization reaction, coordination reaction, aldehyde ketones reaction, reduction reaction and acylation reaction (Scheme 1) [8, 22-27]. The detonation properties of those derivatives, such as 1-amino-2-nitroguanidinium nitrate (ANGN) (*D* = 9775 m s^{-1}, *P* = 43.0 GPa), 1-amino-2-nitroguanidinium 2,4,5-trinitroimidazole salt (*D* = 8398 m s^{-1}, *P* = 30.2 GPa) and aminonitroguanidinium (*D* = 8392.1 m s^{-1}, *P* = 30.71 GPa), are excellent [8, 27, 28], indicating that the energetic derivatives of ANQ have application potential.

Based on much previous work, we designed and obtained three new energetic derivatives of ANQ [1-(2,4-Dinitroanilino)-2-nitroguanidine (DNNG), 1-(2,4,6-Trinitroanilino)-2-nitroguanidine (TNNG) and 1-Amino-2-nitroguanidine-3,5-dinitrosalicylic salt (ANQ·DNS)] through molecular integration of known energetic materials and explored their properties, which will further enrich the research on guanidine compounds.

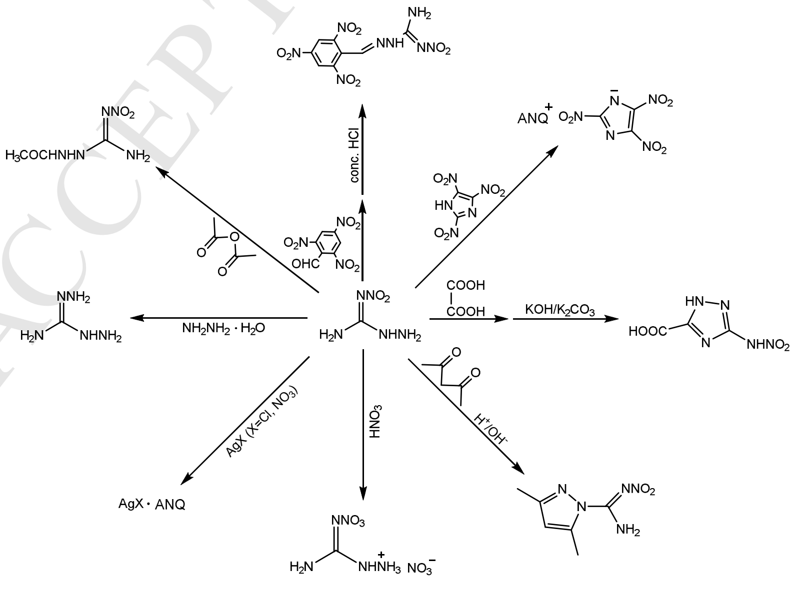

Scheme 1. Different reaction types of ANQ.

2. Experimental

2.1. Materials

2,4-Dinitrochlorobenzene (DNCB) and 2,4,6-trinitrochlorobenzene (TNCB) were obtained from the Xi'an Modern Chemistry Research Institute, and their purity was over 99%. 3,5-Dinitrosalicylic acid (DNS) was analytical-grade commercial product. ANQ was prepared according to Ref. 15.

2.2. Preparation

1-(2,4-Dinitroanilino)-2-nitroguanidine (DNNG) was synthesized according to the following method: ANQ (0.36 g, 3 mmol), DNCB (0.6 g, 3 mmol), KF (0.18 g, 3 mmol) and triethylamine (0.31 g, 3 mmol) were dissolved in anhydrous ethanol (10 mL). After reacting with stirring at 80 °C for 7 h, the resulting solution was slowly cooled to ambient temperature, filtered, washed with water and anhydrous ethanol and dried under vacuum to obtain brown powder of DNNG. Yield: 0.29 g (32.6%). ^{13}C NMR (DMSO-d_6, 500 MHz) δ (ppm): 161.38, 148.65, 137.75, 131.93, 130.73, 123.08, 115.12. ^{1}H NMR (DMSO-d_6, 500 MHz) δ (ppm): 10.19, 9.32, 8.86, 8.38, 7.53, 4.68. IR (KBr, cm^{-1}): 3338, 3280, 3223, 3185, 3007, 2928, 1654, 1569, 1482, 1416, 1386, 1370, 1301, 1167, 1152, 1133, 1040, 1023. Anal. calcd. (%) for $C_7H_7N_7O_6$: C 29.48, H 2.47, N 34.38; found: C 29.18, H 3.07, N 34.68.

1-(2,4,6-Trinitroanilino)-2-nitroguanidine (TNNG) was synthesized according to the following method: ANQ (0.36 g, 3 mmol), TNCB (0.75 g, 3 mmol), KF (0.2 g, 3 mmol) and imidazole (0.31 g, 3 mmol) were dissolved in anhydrous ethanol (10 mL), and the reaction mixture was stirred at 50 °C for 7 h. Then the solution was cooled to ambient temperature slowly, and the resulting solid was filtered off, washed with water and anhydrous ethanol, and dried under vacuum to obtain tan powder of TNNG. Yield: 0.33 g (33.1%). ^{13}C NMR (DMSO-d_6, 500 MHz) δ (ppm): 161.82, 141.75, 140.70, 136.36, 125.21. ^{1}H NMR (DMSO-d_6, 500 MHz) δ (ppm): 9.36, 9.16, 8.99, 4.79. IR (KBr, cm^{-1}): 3393, 3268, 3051, 3036, 1621, 1596, 1533, 1437, 1346, 1256, 1162, 1083, 1014, 929. Anal. calcd. (%) for $C_7H_6N_8O_8$: C 25.46, H 1.83, N 33.94; found: C 25.04, H 2.43, N 34.07.

1-Amino-2-nitroguanidine-3,5-dinitrosalicylic salt (ANQ·DNS) was synthesized according to the following method: ANQ (0.36 g, 3 mmol) and DNS (0.69 g, 3 mmol) were successively dissolved in water (10 mL), and the reaction mixture was stirred at 80 °C for 3 h. After cooling the solution to ambient temperature slowly, yellow needle crystals with crystal water which was identified as ANQ·DNS·3H_2O precipitated. Then ANQ·DNS·3H_2O was dried under vacuum to obtain desiccated anhydrous ANQ·DNS. Yield: 0.98 g (81%). ^{13}C NMR (DMSO-d_6, 500 MHz) δ (ppm): 169.10, 167.41, 160.16, 139.09, 131.13, 130.49, 126.05, 120.76. ^{1}H NMR (DMSO-d_6, 500 MHz) δ (ppm): 9.48, 8.92, 8.68, 8.29, 7.19, 4.43. IR (KBr, cm^{-1}): 3593, 3412, 1663, 1586, 1524, 1453, 1344, 1255, 1178, 1087, 1014, 922, 786. Anal. calcd. (%) for $C_8H_9N_7O_9$: C 27.67, H 2.61, N 28.24; found: C 27.54, H 3.44, N 29.12.

2.3. Physical measurements

NMR spectra were recorded with an AV500 NMR spectrometer (Bruker). IR spectra were determined on NEXUS870 with KBr pellets. Elemental analyses were performed on a Vario EL Ш elemental analyzer. The differential scanning calorimetry (DSC) curves under the condition of flowing nitrogen gas were obtained by DSC200 F3 apparatus over the range of 30 to 350 ºC at heating rates of 10, 15 and 20 ºC min^{-1} respectively. The combustion energy was determined by using an IKA C5000 oxygen-bomb calorimeter (Germany). The thermogravimetry/differential thermogravimetry (TG/DTG) experiments were determined using a SDT-Q600 apparatus (TA, USA) under a nitrogen atmosphere at a flow rate of 100 mL min^{-1}, and the heating rate was 10.0 ºC min^{-1} from ambient temperature to 350 ºC. The impact sensitivities were determined by a ZBL-B impact sensitivity instrument, and the mass of drop hammer was 2.0 kg. The sample mass for each test was 50 mg.

2.4. Crystal structure determinations

Single crystal X-ray diffraction data were collected on a Bruker SMART APEX CCD X-ray diffractometer using graphite-monochromated Mo-Kα radiation (λ = 0.071073 nm). The structure was solved by the direct methods (*SHELXS-97*) and refined by the full-matrix-block least-squares method on F^2 with anisotropic thermal parameters for all non-hydrogen atoms [29-30]. H atoms could be generated from a difference Foutier map, but those which are attached to carbon atoms and cannot be found from the difference Foutier map were repositioned geometrically. Crystal data and refinement results are summarized in Table 1. Because the crystal size of ANQ·DNS·3H_2O

obtained is very small, and the three crystal waters easily lose in the determination process, which can lead to the formation of some disordered structures in the single crystal of ANQ·DNS·3H_2O, the data of ANQ·DNS·3H_2O is not good and its R_1 and wR_2 values are relatively high.

Table 1

Crystal data and structure refinement for TNNG and ANQ·DNS·3H_2O.

Compound	TNNG	ANQ·DNS·3H_2O
Formula	$C_7H_6N_8O_8$	$C_8H_{15}N_7O_{12}$
Formula weight	330.20	401.27
Crystal system	Monoclinic	Triclinic
Space group	$P2_1/c$	P-1
a (Å)	7.9463(17)	6.606(6)
b (Å)	8.8839(19)	10.031(9)
c (Å)	17.848(4)	12.613(11)
α (°)	90	90.476(17)
β (°)	99.092(4)	90.449(19)
γ (°)	90	101.407(18)
V (Å^3)	1244.1(5)	819.3(13)
Z	4	2
Collection T (K)	296(2)	296(2)
D_{calcd} (g cm^{-3})	1.763	1.627
Absorption coefficient (mm^{-1})	0.161	0.153
F (000)	672	416
Crystal size (mm)	0.39×0.21×0.19	0.20×0.10×0.10
θ range (°)	2.311 to 25.781	1.615 to 23.012
Range h, k, l	-5/9, -10/10, -21/18	-7/7, -11/10, -8<13
No. total refln.	6414	3166
No. unique refln.	2388	2214
Comp. to θ_{max} (%)	99.9%	97.7%
Max/min transmission	0.970/0.960	0.985/0.982
Data/restraints/parameters	2388/35/230	2214/46/243
Goodness of fit/F^2	1.018	1.079
Final R	R_1 = 0.0431	R_1 = 0.2016
[$I > 2\sigma(I)$]	wR_2 = 0.0969	wR_2 = 0.3796
R indices (all data)	R_1 = 0.0661	R_1 = 0.3352
	wR_2 = 0.1084	wR_2 = 0.4388
Largest diff. peak/hole (e Å^{-3})	0.218 and -0.298	0.643 and -0.449

3. Results and discussion

3.1. Synthetic reactions

The synthesis routes of the three derivatives of ANQ are shown in Scheme 2. ANQ is an amphoteric compound because of the presence of the electron-withdrawing nitro group and the electron-donating hydrazine group. ANQ possesses high reactivity, especially to its hydrazine group. Based on the nucleophilic substitution reaction of ANQ, two new compounds (DNNG and TNNG) have been obtained through molecular integration in this work. The initiator is the key to these reactions. In this work, imidazole and triethylamine were used to neutralize the acid produced by the reaction and keep the reaction going. Because of the steric hindrance, triethylamine has relatively weak nuclear affinity and can avoid a nucleophilic reaction with the raw materials. However, imidazole has also be proved to be a proper acid binding agent. In addition, the reactions have higher efficiency under anhydrous conditions. Compared to the reaction of ANQ and DNCB at 80 ºC, the reaction between ANQ and TNCB at a lower temperature (50 ºC) can occur successfully. The reason should be that TNCB has three nitro groups bonded to phenyl ring, which makes it possesses stronger electrophilic activity than DNCB. Moreover, we intended to use DNS and ANQ to synthesize another nucleophilic substitution product under similar reaction conditions, but the result was entirely different. An organic ionic salt (ANQ·DNS) was obtained in water as a result of the alkalinity of ANQ and the acidity of DNS.

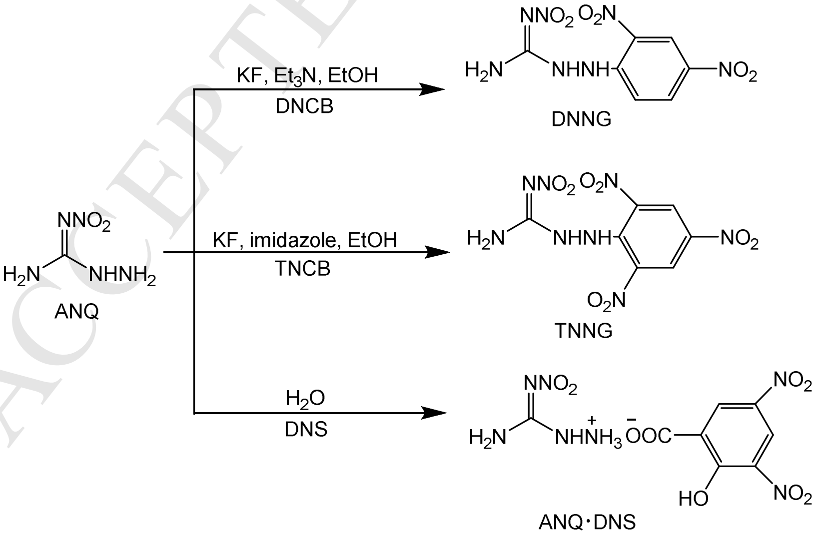

Scheme 2. Synthesis routes of the three derivatives of ANQ.

3.2. NMR and IR spectroscopy

The ^1H NMR spectra of the three compounds show a similar C-NH_2 signal at around 4.5 ppm

(4.68 ppm for DNNG, 4.79 ppm for TNNG and 4.43 ppm for ANQ·DNS), which is in good agreement with that of ANQ (4.67 ppm) [21]. The ^{1}H signals at 8.29 and 9.48 ppm (NH-NH) of ANQ·DNS is in good agreement with that of ANQ (8.27 and 9.32 ppm) [21], but they are shifted to slightly lower field in DNNG (9.32 and 10.19 ppm) and TNNG (9.16 and 9.36 ppm) because of the electron-withdrawing effect of the nitro groups. In addition, the ^{1}H signals of H atoms on the benzene ring of the three compounds are 7.53, 8.38 and 8.86 ppm for DNNG, 8.99 ppm for TNNG, 8.68 and 8.92 ppm for ANQ·DNS, which correspond well with the calculated values (7.42, 8.38 and 8.50 ppm for DNNG, 8.89 ppm for TNNG, 8.96 and 9.09 ppm for ANQ·DNS), and there is also a OH signal (7.19 ppm) in the ^{1}H NMR spectra of ANQ·DNS. The ^{13}C NMR spectra of the three compounds show a similar $C=NNO_2$ signal at around 161 ppm, which is in good agreement with that of ANQ (162 ppm) [21]. The ^{13}C signals at 169.10 ppm (COO) of ANQ·DNS is in agreement with the calculated value (171.8 ppm). Besides, all the ^{13}C signals of C atoms on the benzene ring of the three compounds correspond with their structure.

Because there are many kinds of groups in the three compounds, their IR spectra are relatively complex. The IR spectra of the three compounds all exhibit one N-H stretching band at around 3200-3400 cm^{-1} (3338, 3280 and 3223 cm^{-1} for DNNG, 3393 and 3268 cm^{-1} for TNNG, 3412 cm^{-1} for ANQ·DNS), two antisymmetric and symmetric NO_2 stretching bands at around 1550 and 1350 cm^{-1} [1569, 1416 ($N-NO_2$) and 1370 ($C-NO_2$) cm^{-1} for DNNG, 1596, 1437 ($N-NO_2$) and 1346 ($C-NO_2$) cm^{-1} for TNNG, 1586, 1453 ($N-NO_2$) and 1344 ($C-NO_2$) cm^{-1} for ANQ·DNS], and one C=N stretching band at around 1650 cm^{-1} (1654 cm^{-1} for DNNG, 1621 cm^{-1} for TNNG, 1663 cm^{-1} for ANQ·DNS), which are close to those of ANQ [3357, 3280, 1579, 1410 ($N-NO_2$) and 1667 cm^{-1} respectively] [21]. Moreover, there is an obvious O-H stretching band (3593 cm^{-1}) in the IR spectrum of ANQ·DNS.

3.3. Structure characterizations

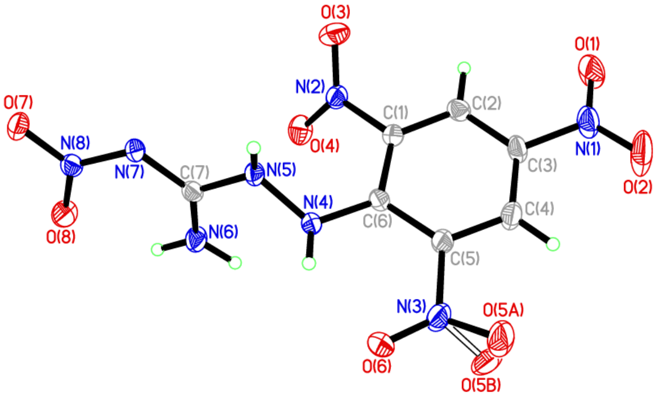

Fig. 1. Crystal structure of TNNG.

Single crystals of TNNG were obtained by solvent evaporation in acetonitrile solution at ambient temperature, and the orderly transparent block crystals of TNNG are yellow. TNNG crystallizes in the monoclinic crystal system with space group $P2_1/c$ containing four molecules per unit cell. As shown in Fig. 1, TNNG exhibits an unsymmetrical structure, and the O(5) atom in the nitro group of TNNG is disordered over two positions with unequal populations for each orientation [the ratio of the occupancy of O(5A) and O(5B) is 0.79:1]. The torsion angles of N(5)-N(4)-C(6)-C(1) (-23.8°) and C(6)-N(4)-N(5)-C(7) (136.8°) indicate that there is a distortion between NH-NH group and benzene ring. However, all non-hydrogen atoms which belong to parent ANQ molecule are approximately coplanar (Table S1), which is consistent with ANQ [21]. This ANQ plane intersects with the benzene ring plane at about 60° (Fig. S1). In addition, the torsion angles between three nitro groups and benzene ring are different. While the nitro group -N(1)O_2 deviate from the benzene ring with only about 10° [O(2)-N(1)-C(3)-C(4) (-11.25°) and O(1)-N(1)-C(3)-C(2) (-10.51°)], there is the biggest torsion with about 50° between the nitro group -N(2)O_2 and benzene ring [C(6)-C(1)-N(2)-O(4) (-49.88°) and C(2)-C(1)-N(2)-O(3) (-51.16°)], which is followed by -N(3)O_2 and benzene ring [O(5A)-N(3)-C(5)-C(4) (29.06°), O(5B)-N(3)-C(5)-C(4) (-34.66°) and O(6)-N(3)-C(5)-C(6) (-8.72°)]. The C(1)-C(6) bond (1.414 Å) and C(5)-C(6) bond (1.413 Å) are longer than other C-C bonds [C(1)-C(2) (1.369 Å), C(2)-C(3) (1.378 Å), C(3)-C(4) (1.362 Å) and C(4)-C(5) (1.381 Å)], indicating that the balance among carbon atoms of the benzene ring has been destroyed by the new substituent. The bond angles of TNNG are distributed around 120° (Table S1), which is relatively uniform and implies it has stable structure.

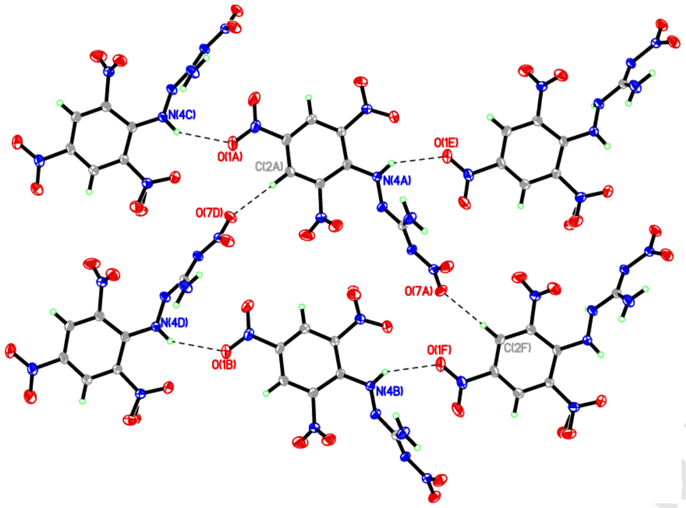

Fig. 2. The 2D network of TNNG showing the intermolecular hydrogen-bond interactions (the dashed lines).

Moreover, there are two kinds of intramolecular hydrogen-bond interactions [N(4)…O(6) (2.627 Å) and N(6)…O(8) (2.561 Å)] in TNNG. Every TNNG molecule is connected to four other by a kind of classical intermolecular hydrogen-bond interactions [N(4)...O(1)#2 (3.457 Å)] and a kind of improper intermolecular hydrogen-bond interactions [C(2)…O(7)#1 (3.277 Å)] to form an infinite 2D network (Fig. 2), then the 2D networks are connected alternately in two directions by three kinds of intermolecular hydrogen-bond interactions [N(5)...O(7)#3 (2.861 Å), N(6)...O(8)#5 (2.910 Å) and N(6)…O(6)#4 (3.141 Å)] to form an infinite 3D framework (Fig. 3) (Table 2).

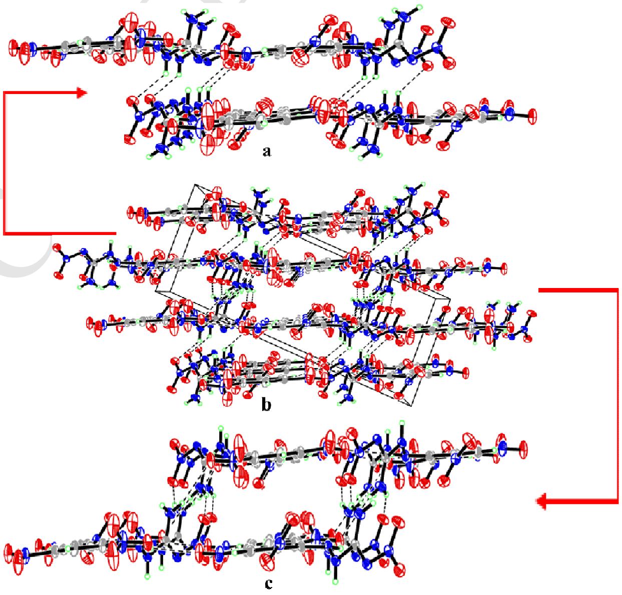

Fig. 3. (**a**) One connection type of two networks of TNNG showing the hydrogen bonds [N(5)...O(7)#3] (the dashed lines). (**b**) The packing of 2D networks of TNNG. (**c**) The other connection type of two networks of TNNG showing the hydrogen bonds [N(6)...O(8)#5 and N(6)…O(6)#4] (the dashed lines).

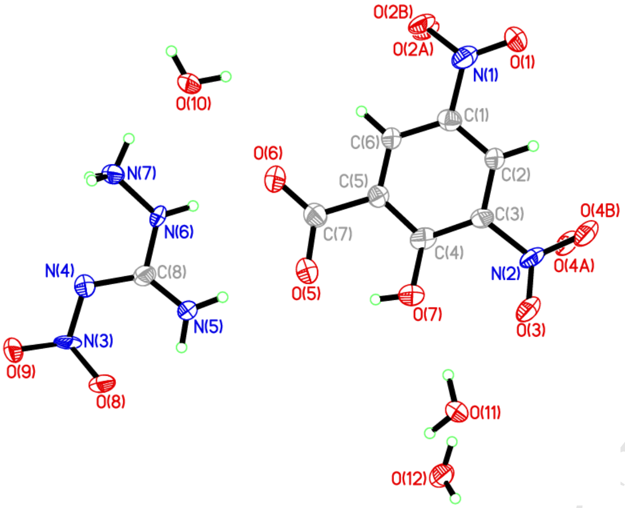

Fig. 4. Crystal structure of $ANQ\cdot DNS\cdot 3H_2O$.

Single crystals of $ANQ\cdot DNS\cdot 3H_2O$ were obtained from the reaction solution. $ANQ\cdot DNS\cdot 3H_2O$ crystallizes in the triclinic crystal system with space group *P*-1 containing two $ANQ\cdot DNS\cdot 3H_2O$ units per unit cell. As shown in Fig. 4, one $ANQ\cdot DNS\cdot 3H_2O$ unit consists of one ANQ^+ cation, one DNS^- anion and three H_2O molecules. The O(2) and O(4) atoms in $ANQ\cdot DNS\cdot 3H_2O$ are split into two atoms [O(2A) and O(2B), O(4A) and O(4B)], respectively, because of the disorder (the ratios of the occupancy of O(2A) to O(2B) and O(4A) to O(4B) are 2.63:1 and 1.18:1 respectively). Not only are all non-hydrogen atoms of ANQ^+ coplanar, which is consistent with ANQ [21], but also ANQ^+ and DNS^- are almost in one plane (Table S2) (Fig. S2). In the ANQ^+ cation, the length of N(4)-C(8) bond (1.384 Å) and N(6)-C(8) bond (1.403 Å) is close to that of normal conjugated N-C double bond (1.34-1.38 Å) and normal N-C single bond (1.47-1.50 Å) [31], respectively, but the length of N(5)-C(8) bond (1.271 Å) is obviously shorter than that of the normal N-C single bond (1.47-1.50 Å) and the length of N(7)-N(6) bond (1.411 Å) is close to that of N(6)-C(8) bond (1.403 Å), which should be attributed to the tautomerism of ANQ and the effect of DNS^- anion. In the DNS^- anion, the length of O(5)-C(7) bond (1.288 Å) and O(6)-C(7) bond (1.240 Å) is close to that of normal C-O double bond (1.21-1.23 Å) and normal C-O single bond (1.30 Å) of carboxylate radical [31], respectively.

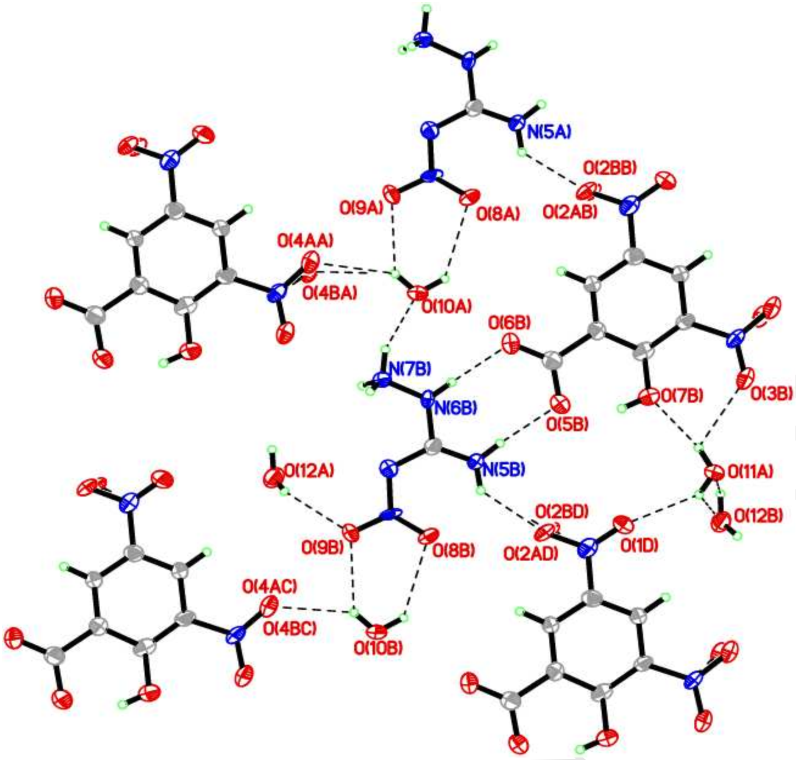

Fig. 5. The 2D network of TNNG showing the hydrogen-bond interactions (the dashed lines).

However, there are many intramolecular and intermolecular hydrogen-bond interactions in the 2D network of ANQ·DNS·$3H_2O$ because of the existence of crystal water (Fig. 5) (Table 2). The 2D networks of ANQ·DNS·$3H_2O$ are connected alternately in two directions by four kinds of intermolecular hydrogen-bond interactions [N(6)...O(2B)#7 (3.040 Å), N(7)...O(11)#8 (2.782 Å), N(7)…O(12)#9 (2.721 Å) and O(12)…O(9)#12 (2.774 Å)] to form an infinite 3D framework (Fig. 6) (Table 2).

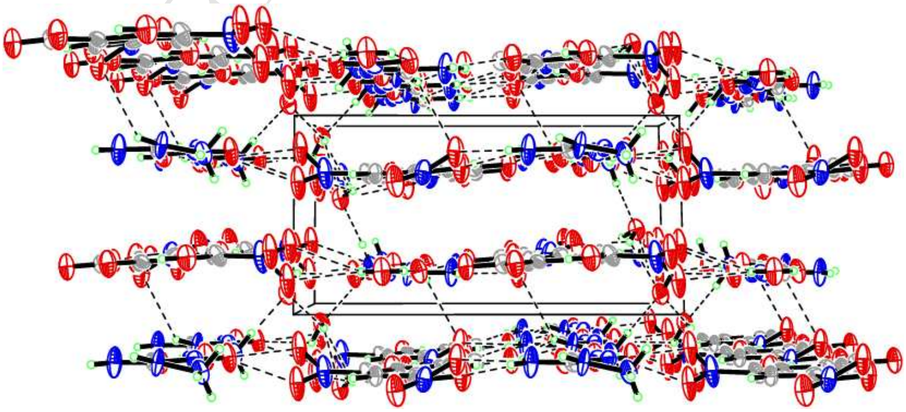

Fig. 6. The packing of ANQ·DNS·$3H_2O$ showing the hydrogen bonds between the 2D networks (the dashed lines).

Table 2

Hydrogen bond interactions in TNNG and ANQ·DNS·3H_2O.

D-H…A	*d*(D—H) / Å	*d*(H…A) / Å	*d*(D…A) / Å	∠DHA / (º)
TNNG				
C(2)-H...O(7)#1	0.93	2.36	3.277(3)	170
N(4)-H...O(1)#2	0.858(15)	2.418(18)	3.157(2)	144.8(19)
N(4)-H...O(6)	0.858(15)	1.964(19)	2.627(2)	133(2)
N(5)-H...O(7)#3	0.873(15)	2.217(19)	2.861(2)	130.4(18)
N(6)-H...O(6)#4	0.896(16)	2.46(2)	3.141(3)	133.6(19)
N(6)-H...O(8)	0.896(16)	1.94(2)	2.561(2)	125(2)
N(6)-H...O(8)#5	0.888(16)	2.078(18)	2.910(3)	156(2)
ANQ·DNS·3H_2O				
N(5)-H...O(2A)#6	0.86	2.17	2.816(18)	131.6
N(5)-H...O(2B)#6	0.86	2.25	2.880(7)	131.0
N(5)-H...O(8)	0.86	1.98	2.555(14)	123.4
N(5)-H...O(5)	0.86	2.05	2.901(14)	169.7
N(6)-H...O(2B)#7	0.86	2.54	3.040(16)	118.7
N(6)-H...O(6)	0.86	2.06	2.835(14)	148.6
O(7)-H...O(5)	0.82	1.69	2.435(13)	150.0
N(7)-H...O(11)#8	0.89	1.89	2.782(16)	175.8
N(7)-H...O(12)#9	0.89	1.83	2.721(15)	176.1
N(7)-H...O(10)	0.89	1.88	2.721(12)	156.3
O(10)-H...O(8)#10	0.85	2.50	3.161(13)	135.8
O(10)-H...O(9)#10	0.85	2.33	2.996(13)	135.0
O(10)-H...O(4A)#11	0.85	2.47	3.160(2)	139.4
O(10)-H...O(4B)#11	0.85	2.40	3.090(2)	138.8
O(11)-H...O(7)	0.85	2.01	2.850(13)	167.8
O(11)-H...O(3)	0.85	2.42	2.927(15)	118.7
O(11)-H...O(1)#6	0.85	2.23	2.895(13)	134.8
O(11)-H...O(12)	0.85	2.19	2.753(14)	123.7
O(12)-H...O(11)	0.85	2.23	2.753(14)	119.4
O(12)-H...O(9)#12	0.85	2.21	2.774(14)	123.9

Symmetry transformations: #1: x+1/2, -y+1/2, z+1/2; #2: x-1/2, -y+3/2, z-1/2; #3: -x+3/2,y+1/2,-z+1/2; #4: -x+1/2, y-1/2, -z+1/2; #5: -x+1/2, y+1/2, -z+1/2; #6: x, y+1, z; #7: -x, -y, -z+1; #8: -x+1, -y+1, -z+1; #9: -x, -y+1, -z+1; #10: x, y-1, z; #11: x, y, z-1; #12: x, y, z+1.

3.4. Thermal behavior

In order to explore the properties of ANQ·DNS itself, the crystals ANQ·DNS·3H_2O with crystal water were dried to obtain desiccated anhydrous ANQ·DNS. The typical TG/DTG curves for DNNG, TNNG and anhydrous ANQ·DNS were obtained (Fig. 7). The TG/DTG curves of DNNG and TNNG are similar and both consist of one intense decomposition stage. The decomposition stage of DNNG occurs in the temperature range of 169.3-178.7 ºC with a mass loss of about 62.90%, and TNNG decomposes in the temperature range of 163.5-178.2 ºC with a mass loss of about 62.96%. However, the TG/DTG curves of anhydrous ANQ·DNS contain two mass loss processes. The first process of anhydrous ANQ·DNS is a small decomposition process occurring at 120.6-162.3 ºC with a mass loss of about 18.57%, and the second process is a big and long decomposition process occurring at 190.1-292.7 ºC with a mass loss of about 54.14%.

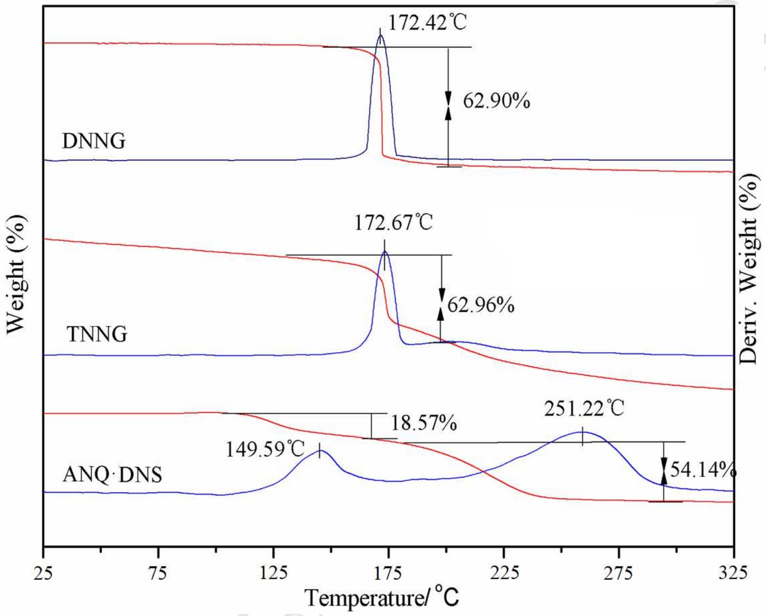

Fig. 7. TG/DTG curves of the three compounds at a heating rate of 10 °C min^{-1}.

The typical DSC curves for DNNG, TNNG and anhydrous ANQ·DNS were also obtained (Fig. 8), and ANQ·DNS·3H$_2$O were also measured by DSC to explore the effect of crystal water on ANQ·DNS. The DSC curves for DNNG and TNNG show only one intensely exothermic peak, which is consistent with their TG/DTG curves. and the extrapolated onset temperatures, peak temperatures and decomposition enthalpy are 172.12 ºC, 175.78 ºC, 743 J g^{-1} and 168.23 ºC, 169.62 ºC, 663 J g^{-1}, respectively. However, the DSC curves of ANQ·DNS·3H$_2$O and ANQ·DNS are completely different from those of DNNG and TNNG. The first stage of ANQ·DNS·3H$_2$O is an endothermic stage at about 63 ºC, which should be the process of losing crystal water because it does not appear in the test of anhydrous ANQ·DNS, and the extrapolated onset temperature, peak temperature and decomposition enthalpy are 54.75 °C, 63.95 °C and -227 J g^{-1}, respectively. The first stage of anhydrous ANQ·DNS is an endothemic stage at about 128 ºC, which should be a melting process of anhydrous ANQ·DNS and cannot be found in the test of ANQ·DNS·3H_2O, and the extrapolated onset temperature, peak temperature and decomposition enthalpy are 125.00 °C, 128.37 °C and -50 J g^{-1}, respectively. In addition, both ANQ·DNS·3H_2O and anhydrous ANQ·DNS present a similar exothermic stage (the extrapolated onset temperature, peak temperature and decomposition enthalpy are 136.19 °C, 151.25 °C and 280 J g^{-1} for ANQ·DNS·3H_2O, and 131.74 °C, 151.37 °C and 438 J g^{-1} for anhydrous ANQ·DNS, respectively), which is consistent with the first decomposition process in the TG/DTG curve of ANQ·DNS, and a similar long endothermic process (the extrapolated onset temperature, peak temperature and decomposition enthalpy are 191.94 °C, 237.12 °C and -233 J g^{-1} for ANQ·DNS·3H_2O, and 190.52 °C, 247.92 °C and -357 J g^{-1} for anhydrous ANQ·DNS, respectively), which corresponds to the second decomposition process in the TG/DTG curve of ANQ·DNS.

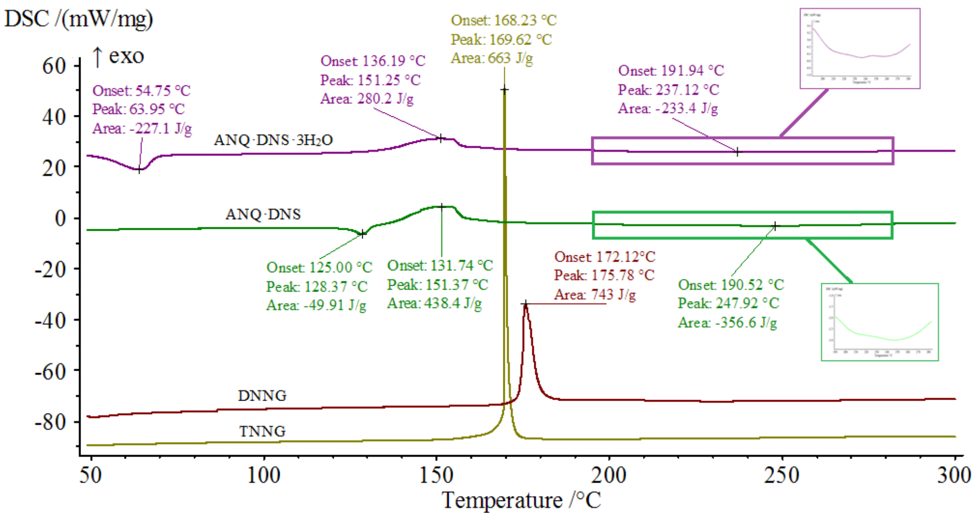

Fig. 8. DSC curves of the three compounds at a heating rate of 10 °C min^{-1}.

From the thermal behaviors of the three compounds, the order of thermal stability for the three compounds is DNNG > TNNG > ANQ·DNS. However, they are all more unstable than ANQ which present only one exothermic decomposition peak at around 193-196 °C [21]. For the salt ANQ·DNS, its thermal behavior is significantly different from that of ANQ and the other two compounds, which should be attributed to the effect of ionic bonding force and the hydrogen bonds.

A multiple heating method (Kissinger method [32] and Ozawa method [33]) was employed to obtain the kinetic parameters [the apparent activation energy (*E*) and pre-exponential factor (*A*)] of the exothermic decomposition reaction for the three compounds. The measured values of extrapolated onset temperature (T_e) and peak temperature (T_p) of the exothermic decomposition reaction are listed in Table 3. The above-mentioned E and A values and linear correlation coefficients (r) are also listed in Table 3. The results indicate that the apparent activation energy obtained by Kissinger method agrees well with that obtained by Ozawa method, and the linear correlation coefficients (r) are all very close to 1, so the results are credible. Moreover, the apparent activation energy of the exothermic decomposition reaction for ANQ (224.3 kJ mol^{-1}) [21] is higher than that of DNNG (176.1 kJ mol^{-1}), TNNG (130.4 kJ mol^{-1}) and ANQ·DNS (90.7 kJ mol^{-1}), which indicates that DNNG, TNNG and ANQ·DNS are easier to decompose than ANQ. This result corresponds with their thermal stability.

Table 3

The values of T_e, T_p, E_k, log$A$, r_k, E_o and r_o for the three compounds determined by DSC at various heating rates (β).

	β (°C·min^{-1})	T_e (°C)	T_p (°C)	E_k (kJvmol^{-1})	Log (A s^{-1})	r_k	E_o (kJ mol^{-1})	r_o
DNNG	10	172.12	175.78	176.1	18.73	0.99	174.6	0.99
	15	177.26	180.15					
	20	178.93	181.99					
TNNG	10	168.23	169.62	130.4	13.51	0.99	131.1	0.99
	15	174.11	174.29					
	20	177.54	177.99					
ANQ·DNS	10	131.74	151.37	90.7	9.2	0.98	93.1	0.99
	15	139.43	158.98					
	20	144.28	161.76					

Subscript k, data obtained by Kissinger method; subscript o, data obtained by Ozawa method.

The self-accelerating decomposition temperature (T_{SADT}) and critical temperature of thermal explosion (T_b) are two important parameters required to ensure safe storage and process operations for energetic materials and for evaluating their thermal stability, which can be calculated according to Ref. 34-36. T_{SADT} and T_b were calculated as 166.33 and 174.42 °C for DNNG, and 154.08 and 166.14 °C for TNNG, respectively, which is consistent with the DSC analysis. However, the T_{SADT} and T_b values of both DNNG and TNNG are lower than those of ANQ

(T_{SADT}=184.5 °C, T_{b}=192.7 °C) [21]. In addition, because ANQ·DNS contains two decomposition stages, it is difficult to evaluate its T_{SADT} and T_{b}.

3.5. Detonation properties

Detonation velocity (*V*) and detonation pressure (*P*) are two important parameters to evaluate the application performance of energetic materials and can be calculated by the nitrogen equivalent equations and the Kamlet–Jacobs (*K*–*J*) equations [37]. The detonation velocity (*D*), detonation pressure (*P*), impact sensitivities (IS) and other properties of DNNG, TNNG and ANQ·DNS are summarized in Table 4 with those of ANQ, 2,4,6-trinitrotoluene (TNT) and RDX for comparison [38-41]. The results show that the sensitivity of ANQ·DNS is the lowest among the six compounds, but the sensitivities of DNNG and TNNG are relatively high. The detonation properties of DNNG, TNNG and ANQ·DNS are all better than TNT, and their order is TNNG > ANQ·DNS > DNNG. Among these three compounds, TNNG possesses comparable detonation properties to ANQ and RDX, so TNNG has potential value of research and application as primary explosives. In addition, the combustion enthalpy of TNNG was measured as 11486 J g^{-1} (Table S3), and the enthalpy of formation for TNNG is calculated as 156.64 kJ mol^{-1} according to Hess's law.

Table 4

Sensitivity and performance comparison of DNNG, TNNG, ANQ·DNS, ANQ, RDX and TNT.

	M^a (g mol^{-1})	$T_m{}^b$ (°C)	d^c (g cm^{-3})	N^d (%)	OB^e (%)	IS^f (J)	P^g (GPa)	D^h (km s^{-1})
DNNG	285.18	175	1.63^k	34.38	−64.6	5.4	22.4^i	7.3^i
TNNG	330.17	170	1.77^l	33.94	−43.7	4.0	29.5^i 31.1^j	8.2^i 8.3^j
ANQ·DNS	347.2	128	1.63^l	32.09	−43.5	>40	23.4^i	7.5^i
ANQ	119.08	191	1.72	58.81	−33.6	20	30.7	8.7
RDX	222.12	204.5	1.82	37.84	−21.6	7.4	33.7	8.7
TNT	227.13	80.5	1.65	18.5	−24.6	15	19.5	6.8

[a] Molecular mass. [b] Melting point. [c] Crystal density. [d] Nitrogen content. [e] Oxygen balance. [f] Impact sensitivity. [g] Detonation pressure. [h] Detonation velocity. [i] Based on the nitrogen equivalent equations. [j] Based on the Kamlet–Jacobs (*K*–*J*) equations. [k] Theoretical calculation result. [l] Crystal density.

4. Conclusion

In conclusion, three new compounds based on ANQ were synthesized through molecular integration. The synthesis reactions of DNNG and TNNG were realized by using acid-binding agents (triethylamine and imidazole), and ANQ·DNS was obtained easily in water due to the alkalinity of ANQ and the acidity of DNS. TNNG crystallizes in the monoclinic crystal system with space group $P2_1/c$ containing four molecules per unit cell, and ANQ·DNS·3H_2O crystallizes in the triclinic crystal system with space group P-1 containing two ANQ·DNS·3H_2O units per unit cell. DNNG and TNNG possess similar thermal behaviors and both present only one intense exothermic decomposition process at around 170 °C, but ANQ·DNS shows more complex thermal behaviors. The order of thermal stability for the three compounds and ANQ are ANQ > DNNG > TNNG > ANQ·DNS. The impact sensitivity of ANQ·DNS (>40 J) are very low, but the impact sensitivities of DNNG (5.4 J) and TNNG (4.0 J) are relatively high. The detonation properties of TNNG (D = 8.3 km s^{-1}, P = 31.1GPa) is close to ANQ and RDX. This work further enriches the research on ANQ.

Acknowledgements

The work is supported by the National Natural Science Foundation of China (21673178).

Appendix A. Supporting information

Crystallographic data for the structural analysis have been deposited in the Cambridge Data Center (CCDC). CCDC number: 1574555 for TNNG and 1574566 for ANQ·DNS·3H_2O.

References

[1] Q.L. Yan, A. Cohen, A.K. Chinnam, N. Petrutik, A. Shlomovich, L. Burstein, M.J. Gozin, J. Mater. Chem. A 4 (2016) 18401.

[2] X.H. Jin, B.C. Hu, Z.L.J. Liu, Brazil. Chem. Soc. 26 (2015) 124.

[3] R. Selvakumar, S.J. Geib, A.M. Sankar, T. Premkumar, S.J. Govindarajan, J. Phys. Chem. Solids. 86 (2015) 49.

[4] G.R. Andradea, J. Kunsminskasb, L. Pizzutib, A.D. Anjosc, S.D. Inglezd, B. Tirlonie, P. H. Suegamab, Inorg. Chem. Commun. 61 (2015) 210.

[5] Y. Li, H.F. Huang, X.Y. Lin, R.M. Pan, J. Yang, RSC Adv. 6 (2016) 54310.

[6] R.S. Damse, J. Hazard. Mater. 172 (2009) 1383.

[7] S.R. Naidu, K.V. Prabhakaran, N.M. Bhide, E.M. Kurian, J. Therm. Anal. Calorim. 61 (2000) 861.

[8] X.H. Jin, B.C. Hu, Z.L. Liu, C.X. Lv, RSC Adv. 4 (2014) 23898.

[9] M. Mahdavi, K. Ghani, K. Nosratzadegan, Z. Anorg. Allg. Chem. 643 (2017) 1771.

[10] G. Todde, S.K. Jha, G. Subramanian, M.K. Shukla, Surf. Sci. 668 (2018) 54.

[11] T. Templea, M. Ladymana, N. Maia, E. Galantea, M. Ricamoraa, R. Shirazia, F. Coulonb, Sci. Total. Environ. 625 (2018) 1264.

[12] R. Phillips, J.F. Williams, J. Am. Chem. Soc. 50 (1928) 2465.

[13] R.A. Henry, R.C. Makosky, G.B.L. Smith, J. Am. Chem. Soc. 73 (1951) 474.

[14] A.F. Mckay, Chem. Rev. 51 (1952) 301.

[15] J.A. Castillo-Meléndez, B.T. Golding, Synthesis 10 (2010) 1655.

[16] N. Fischer, T.M. Klapötke, K. Lux, F.A. Martin, J. Stierstorfer, Crystals 2 (2012) 675.

[17] N. Fischer, T.M. Klapötke, J.Z. Stierstorfer, Zeitschrift für Naturforschung B 67 (2012) 573.

[18] T.M. KlapOtke, J. Stierstorfer, Proceedings of the 27th Army Science conference, Orlando, FL, USA, 2010.

[19] T.M. Klapötke, J. Stierstorfer, Insensitive Munitions Energetic Materials Technology Symposium, Germany, 2010.

[20] G.Q. Zhang, X.B. Liu, M. Huang, Chin. J. Energ. Mater. 21 (2013) 668.

[21] Y. Li, M. Wang, K. Xu, J. Song, F. Zhao, Chin. J. Energ. Mater. 24 (2016) 848.

[22] B. Wu, H.W. Yang, Y.X. Tang, Z.X. Wang, C.X. Lu, G.B. Cheng, J. Energ. Mater. 33 (2015) 180.

[23] E. Lieber, E. Sherman, R.A. Henry, J. Cohen, J. Am. Chem. Soc. 73 (1951) 2327.

[24] O.Y. Ozerova, T.P. Efimova, T.A. Novikova, V.V. Gurzhii, V.M. Berestovitskaya, Russ. J. Gen. Chem. 85 (2015) 1623.

[25] N. Fischer, M. Joas, T.M. Klapötke, J. Stierstorfer, Inorg. Chem. 52 (2013) 13791.

[26] R. A. Henry, J. Am. Chem. Soc. 72 (1950) 5343.

[27] X.H. Jin, B.C. Hu, Z.L. Liu, J. Brazil. Chem. Soc. 26 (2015) 124.

[28] Q.Q. Liu, B. Jin, R.F. Peng, Z.C. Guo, J. Zhao, Q.C. Zhang, Y. Shang, J. Mater. Chem. A 4 (2016) 4971.

[29] G. M. Sheldrick, SHELXS-97, Program for crystal structure refinement, University of Göttingen, University of Göttingen, Germany, 1997.

[30] G. M. Sheldrick, SHELXL-97, Program for crystal structure refinement, University of Göttingen, Germany, 1997.

[31] X. M. Chen, J. W. Cai, Single-Crystal Structure Analysis-Principles and Practices, Science Press, Beijing, second ed., 2007.

[32] H. E. Kissinger, Anal. Chem. 29 (1975) 1702.

[33] T. B. Ozawa, Chem. Soc. Jpn. 38 (1965) 1881.

[34] R. Z. Hu, S. L. Gao, F. Q. Zhao, Q. Z. Shi, T. L. Zhang, J. J. Zhang, Thermal Analysis Kinetics 2nd Ed., Science Press, Beijing, 2008.

[35] S. Vyzovkin, A. K. Burnham, J. M. Criado, L. A. Maqueda, C. Popescu, N. Sbirrazzuoli, Thermochim. Acta. 520 (2011) 1.

[36] T. L. Zhang, R.Z. Hu, Y. Xie, F. P. Li, Thermochim. Acta. 244 (1994) 171.

[37] M. J. Kamlet, S. J. Jacobs, J. Chem. Phys. 48 (1968) 23.

[38] J. M. Shreeve, T. T. Vo, J. Mater. Chem. A 3 (2015) 8756.

[39] T. H. Zhou, Y. F. Li, K. Z. Xu, J. R. Song, F. Q. Zhao, New J. Chem. 41 (2017) 168.

[40] Y. D. Tian, F. Q. Zhao and J. H. Liu, Handbook of Energetic Materials and the Related Compounds, National Defense Industry Press, Beijing, 2011. (in Chinese)

[41] Y. H. Joo, H. X. Gao, D.A. Parrish, S.G. Cho, E. M. Gohd, J. M. Shreeve, J. Mater. Chem. 22 (2012) 6123.

Highlights:

- Three new energetic compounds based on ANQ were synthesized and characterized.
- Crystal structures of two compounds were determined and discussed.
- Thermal behaviors of three compound were described.
- Detonation properties of TNNG are close to ANQ and RDX.